

## Comparison of Soil Pollution Due To E-Waste Pollutants at Two Dumpsites in Lagos State Using the Geophysical Assessment Method

Paul Adeniran Ajakaye<sup>a</sup>, Somoye Emmanuel<sup>b</sup>, Owolabi Lawal<sup>c</sup>

<sup>a</sup>Center for Environmental Study and Sustainable Development, Lagos State University, Ojo, Lagos, Nigeria

<sup>b</sup>Department of Physics, Lagos State University, Ojo, Lagos, Nigeria.

<sup>c</sup>Department of Science and Technology Education, Lagos State University, Lagos, Nigeria.

### \*Corresponding author

Paul Adeniran Ajakaye, Center for Environmental Study and Sustainable Development, Lagos State University, Ojo, Lagos, Nigeria

Submitted: 16 Feb 2022; Accepted: 21 Feb 2022; Published: 02 Mar 2022

**Citation:** Paul Adeniran Ajakaye, Somoye Emmanuel, Owolabi Lawal, (2022). Comparison of Soil Pollution Due To E-Waste Pollutants at Two Dumpsites in Lagos State Using the Geophysical Assessment Method. *Adv Envi Was Mana Rec*, 5 (1), 25-39.

### Abstract

Soil degradation forms a part of the significant impacts arising from indiscriminate disposal of e-waste. This study was aimed at assessing, through the analysis of VES and 2D-Wenner array configuration data, not only the magnitude of legacy contamination by e-waste in terms of depth and spread but the level of impact as a result of the soil type or nature. The results of the VES data and 2D resistivity analysis showed that Alaba dumpsite was highly impacted by the e-waste due to the permeable geoelectric characteristics of the lithologic units beneath the dumpsite while Soulous- Igando recorded relatively high resistivity values which correspond to the clay column identified in the geoelectric sections of the site, thus the level of soil impact was low because, the clay/laterite column of the subsurface of Soulous-Igando site provides a means of preventing leachate movement down to the aquifer. The sites might need to be recovered in the future for a better developmental project; hence, the benefits of this research on the appropriate methods to detoxify the sites. In addition, the results from this study could facilitate Lagos State Government decisions on improving protection for groundwater resources for residents around the study area.

**Keywords:** E-waste, Geoelectric, Geophysical, Lithologic, Resistivity, VES, 2D-Wenne

### Introduction

Soil serves as a very important sink for heavy metal contaminants in an ecosystem [1]; so its pollution by heavy metals is a problem of concern considering the adverse consequences on plant, animal and human [2]. According to Balseiro-Romero and Baveye [3]; Jerzy et al., [4] and Xudong et al., [5]; “heavy metals, due to the mobility of the pollutants in deep soil, may result in groundwater contamination either as a result of natural or manmade processes”.

Several studies including Ofudje et al., [6]; Adeyi and Oyeleke had revealed the impact of e-wastes on dumpsites soil through the detection of high concentrations of heavy metals like Cr, Cu, Zn, Ni, and Mn in the soil although in some instances the concentrations were found to be below the stipulated standard limits [7]. The probable reasons for the different conclusions have been attributed to age of the dumping sites and level of activities in terms of indiscriminate burning, melting or chemical leaching of e-waste by informal operators or scavengers at the sites [7]. However, the studies fell short of recognising the contribution of the dumpsite type of soil to the migration of leachate in the soil leading to the eventual contamination of groundwater.

The aim of this study is to investigate the effects of dumpsite type of soil on the level of impacts of the soil due to indiscriminate dumping of e-wastes. Two different open dumpsites locations at Alaba International Market and Solous - Igando, Lagos, Nigeria.

### Field description

The first site has been in existence for more than 20 years as a dumpsite where e-waste collectors and recyclers work, live in sheds and indulge in burning and other crude methods of recycling in an attempt to extract valuable components of e-waste. It is located at Alaba International Market, Ojo Local Government Area, Lagos State, Nigeria.

The second site is located at Soulous-Igando dumpsite in the South Western part of Lagos State along LASU – Isheri Road in Alimosho Local Government. It started operations more than 25 years ago and it receives waste of all sorts including e-wastes, other domestic, commercial, industrial and institutional trashes from entire Lagos State [8]. The base maps of the locations are shown in Figure. 1.

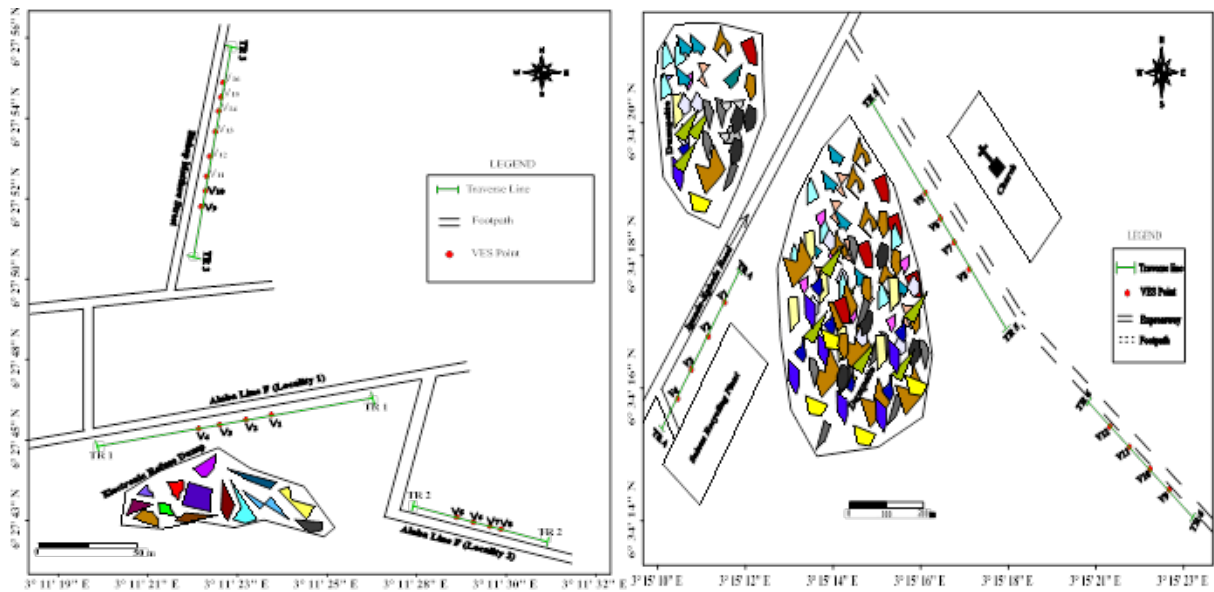


**Figure 1:** Base map for Alaba International Market and Soulous-Igando dumpsites

### Local Geology/Geomorphology of Lagos State

Lagos State lies within the geographic coordinates of Lat.: N06° 23' and N06° 40' and Long.: E03° 13' and E03° 27' [9]. It is within the Euro – African sector of the world in the neighbourhood of the Greenwich Meridian [10]. Experts have described the local geology/geomorphology of Lagos State as follows; Lagos is underlain by the Dahomey Basin with lithologic constituents that are mainly sands, clays and limestones. The basement complex which forms the basement rocks in the basin is overlain in succession by the Cretaceous Abeokuta Formation which is sandy with inter-bedded shales and limestone formation. Following it is the Tertiary Ewekoro Formation comprising of limestone, clays and shales and the Ilaro formation consisting of clays and shales followed by the poorly sorted coastal plain sands and recent alluvial deposits. The latter which consists of lithoral and lagoonal sediments of the coastal belt is characterized by mangrove (saltwater) and freshwater swamps where aquifers, are readily recharged by copious

rainfall thus making them vulnerable to leachate contamination in areas proximal to landfills [11, 12].

### Materials and Methods

Geophysical investigation involving 2-D electrical resistivity imaging (ERI) via Wenner array configuration and 1-D Vertical Electrical sounding adopting Schlumberger array was carried out along predetermined traverses within the study area. The 2-D resistivity data were collected at inter-electrode spacing of 10 m along some traverses and 5 m at other traverses as shown in Table 1. The varied inter-electrode spacing was due to constraint in available space within the study areas which had developed to communities. A total of six traverses were occupied and along each traverse, four VES were acquired at predetermined stations except on traverse three where it was possible to acquire eight VES because of the available space. Thus, 28 VES were acquired in all as shown in Table 1.

**Table 1:** Traverse Spacing and Number of Vertical Electrical Sounding

TRAVERSE	ELECTRODE SPACING (m)	TRAVERSE LENGTH (m)	NO. OF VES	COORDINATE Lat. (N)/Long. (E)
Alaba				
1	10	200	4	60 27' 45.8"/0030 11' 26.5"
2	5	100	4	60 27' 43.6"/0030 11' 27.5"
3	10	200	8	60 27' 50.3"/0030 11' 22.2"
Soulous				
4	5	100	4	60 34' 15.3"/0030 15' 09.8"
5	10	150	4	60 34' 20.6"/0030 15' 15.0"
6	5	100	4	60 34' 13.9"/0030 15' 22.9"

## Results and Discussions

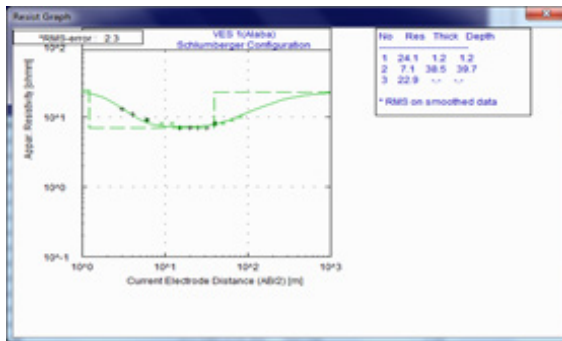
The curve matching (observing the shape of the field curve) method was used to interpret the sub-surface resistivity distribution. A curve is drawn by plotting apparent resistivity against electrode spacing; field curve was then matched with the master curve for qualitative interpretation [13]. Subsequently, the VES data were processed using segment by segment curve matching through which the geoelectric models of the subsurface were generated. The distributions of resistivities of different subsurface layers ( $\rho$ ) were classified, based on curve shapes, in a three-layered earth model divided into four groups (minimum, double ascending, maximum, and double descending types) depending on the relative values of  $\rho_1$ ,  $\rho_2$ , and  $\rho_3$  or a combination of the curves [14, 15]. These models were fed into the Winresist (version 1.0, C.1998, 2004) software along with the field data to undergo iteration and obtain the best fit between the field data and the calculated models

for generating the geoelectric sections of the subsurface along each traverse.

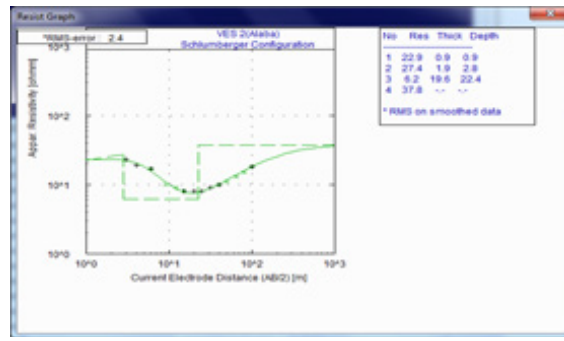
The acquired 2-D resistance data were multiplied by the geometric factor and then fed into Dipprofwin software for inversion and 2-D resistivity images of the subsurface to show the pollutant plumes along the traverses. The results from both 2-D ERI and VES were integrated to determine the extent of impact of pollutants at the e-waste dumpsites in the same manner of investigation by Vasant-rao et al., [15].

### Geoelectric Section (VES) of Alaba dumpsite soil

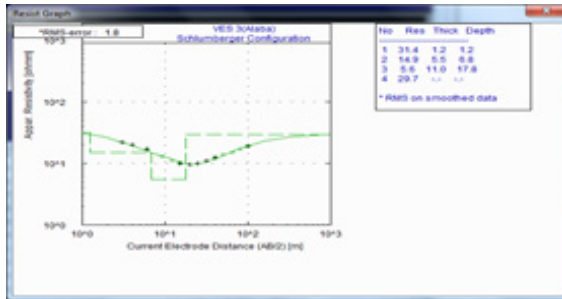
Sounding curve types obtained at Alaba were H, KH, A, HK, QH and K (see Fig. 2 and Table 2). The iteration of these curve types led to the identification of the geoelectrical section or nature of the dumpsite subsurface soil. The summary of the curve types (VES 1 – VES 16) and site lithology is shown in Table 2.



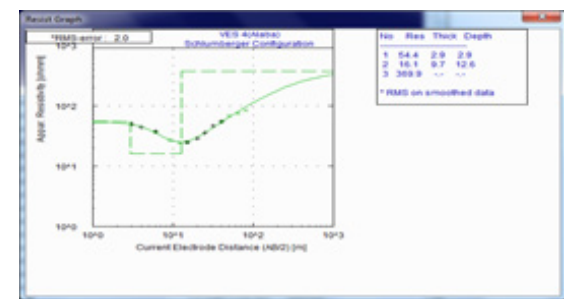
VES 1: H type:  $\rho_1 > \rho_2 < \rho_3$  curve



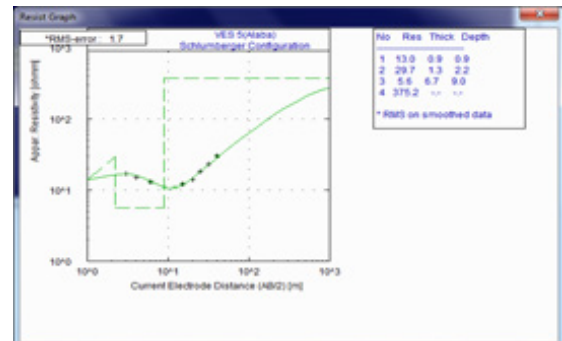
VES 2: KH type:  $\rho_1 > \rho_2 > \rho_3 < \rho_4$  curve



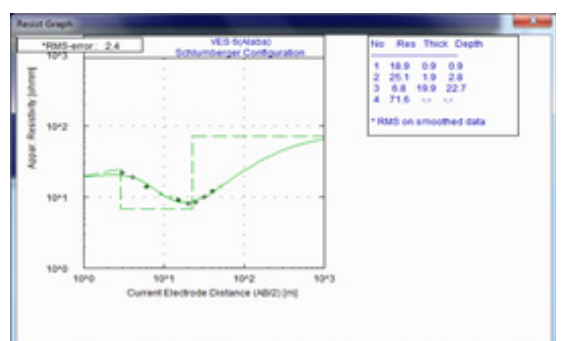
VES 3: KH type:  $\rho_1 > \rho_2 > \rho_3 < \rho_4$  curve



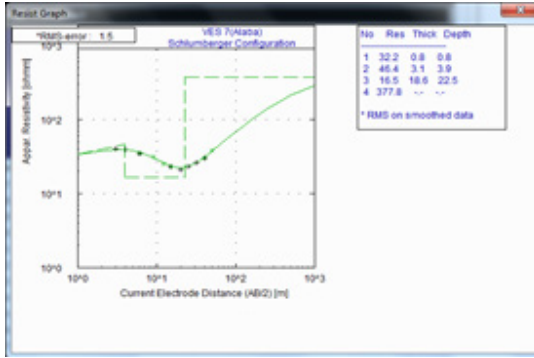
VES 4: H type:  $\rho_1 > \rho_2 < \rho_3$  curve



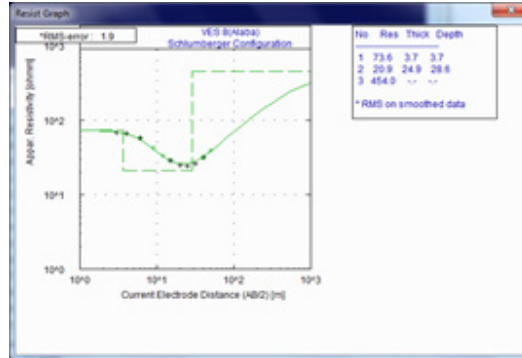
VES 5: KH type:  $\rho_1 > \rho_2 > \rho_3 < \rho_4$  curve



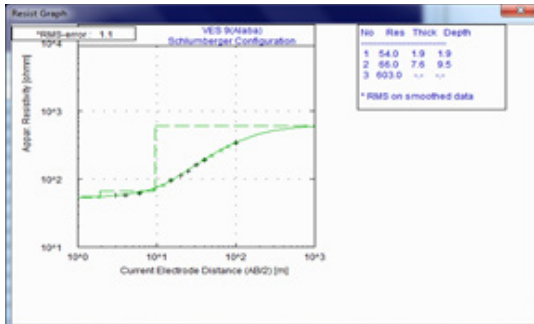
VES 6: KH type:  $\rho_1 > \rho_2 > \rho_3 < \rho_4$  curve



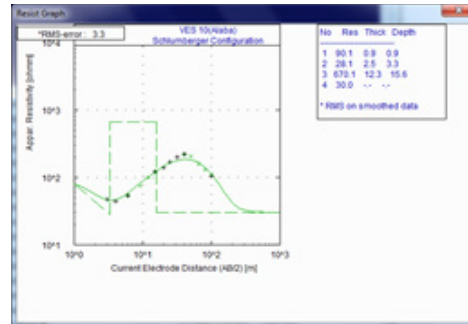
VES 7: KH type:  $\rho_1 > \rho_2 > \rho_3 < \rho_4$  curve



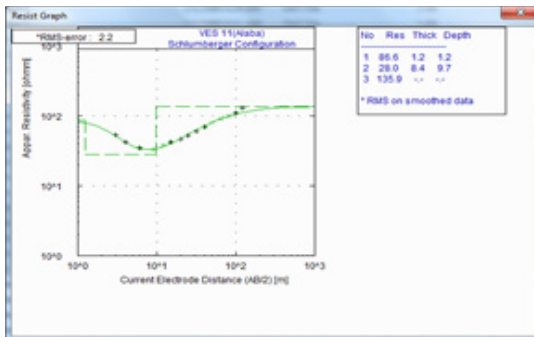
VES 8: H type:  $\rho_1 > \rho_2 < \rho_3$  curve



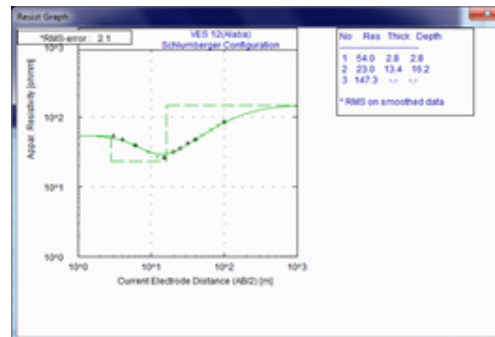
VES 9: A type:  $\rho_1 < \rho_2 < \rho_3$  curve



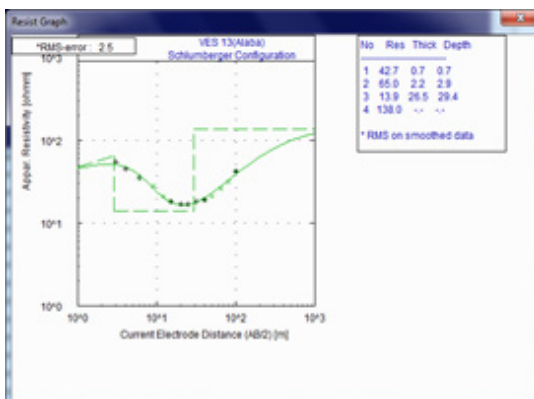
VES 10: HK type:  $\rho_1 > \rho_2 < \rho_3 > \rho_4$  curve



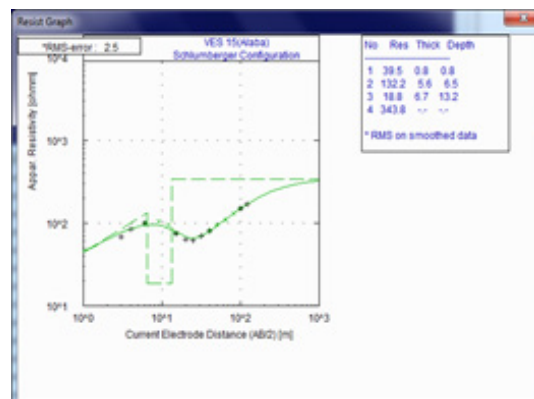
VES 11: H type:  $\rho_1 > \rho_2 < \rho_3$  curve



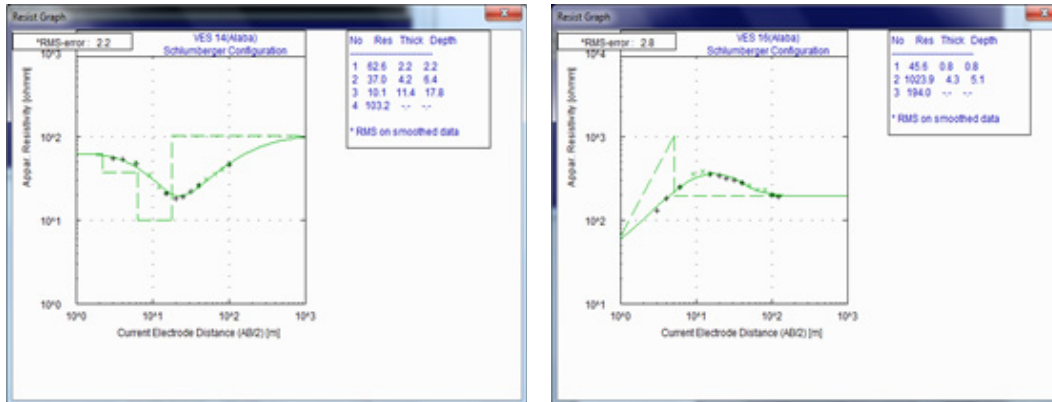
VES 12: H type:  $\rho_1 > \rho_2 < \rho_3$  curve



VES 13: KH type:  $\rho_1 > \rho_2 > \rho_3 < \rho_4$  curve



VES 14: KH type:  $\rho_1 > \rho_2 > \rho_3 < \rho_4$  curve



VES 15: QH type:  $\rho_1 > \rho_2 > \rho_3 < \rho_4$  curve

VES 16: K type:  $\rho_1 < \rho_2 > \rho_3$  curve

**Figure 2:** VES curves 1 – 16 for Alaba international market dumpsite

**Table 2: Vertical Electrical Sounding Summary of Alaba International Market Dumpsite**

VES NO	RESISTIVITY (ohm-m)	THICKNESS (m)	DEPTH (m)	LITHOLOGY	CURVE TYPE
1	24	1.2	1.2	Topsoil	H
	7	38.5	39.7	Leachate	
	23	-----	-----	Clay	KH
2	23	0.9	0.9	Topsoil	
	27	1.9	2.8	Clay	
	6	19.6	22.4	Leachate	
	38	-----	-----	Clay	
3	31	1.2	1.2	Topsoil	KH
	15	5.5	6.8	Clay	
	6	11	17.8	Leachate	
	30	-----	-----	Clay	
4	31	1.2	1.2	Topsoil	H
	54	2.9	2.9	Topsoil	
	16	9.7	12.6	Clay	
	370	-----	-----	Sand	
5	13	0.9	0.9	Topsoil	KH
	30	1.3	2.2	Clay	
	6	6.7	9	Leachate	
	375	-----	-----	Sand	
6	19	0.9	0.9	Topsoil	KH
	25	1.9	2.8	Clay	
	7	20	23	Leachate	
	72	-----	-----	Sandy clay	
7	32	0.8	0.8	Topsoil	KH
	46	3.1	3.9	Sandy clay	
	17	18.6	22.5	Clay	
	378	-----	-----	Sand	



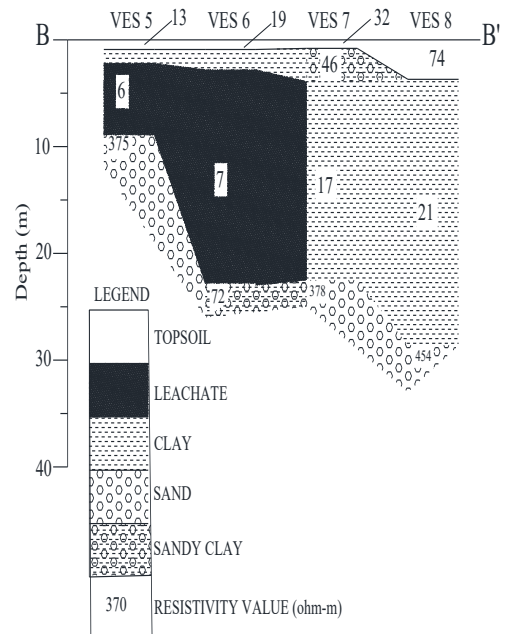
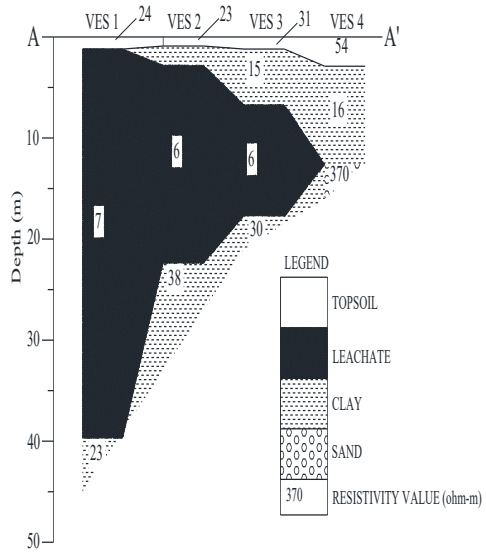
8	74	3.7	3.7	Topsoil	H
	21	24.9	28.6	Clay	
	454	-----	-----	Sand	
9	54	1.9	1.9	Topsoil	A
	66	7.6	9.5	Clayey sand	
	603	-----	-----	Sand	
10	90	0.9	0.9	Topsoil	HK
	28	2.5	3.3	Clay	
	670	12.3	15.6	Sand	
	30	-----	-----	Clay	
11	87	1.2	1.2	Topsoil	H
	28	8.4	9.7	Clay	
	136	-----	-----	Sand	
12	54	2.8	2.8	Topsoil	H
	23	13.4	16.2	Clay	
	147	-----	-----	Sand	
13	43	0.7	0.7	Topsoil	KH
	65	2.2	2.9	Sandy clay	
	14	27	29.4	Clay	
	138	-----	-----	Sand	
14	63	2.2	2.2	Topsoil	QH
	37	4.2	6.4	Clay	
	10	11.4	17.8	Clay	
	103	-----	-----	Sand	
15	40	0.8	0.8	Topsoil	KH
	132	5.6	6.5	Sand	
	19	6.7	13.2	Clay	
	344	-----	-----	Sand	
16	47	0.8	0.8	Topsoil	K
	1024	4.3	5.1	Sand	
	194	-----	-----	Sand	

The results of the vertical electrical sounding (see Figure. 3 a, b, c & d) revealed that the geoelectric section of Alaba dumpsite consists mostly three subsurface layers composed of clay column, clayey sand and sand which allows a high level of impact of the dumpsite soil.

#### Depths and Spread of Pollutants in Alaba Dumpsite Soil Based On the 2d Wenner Array

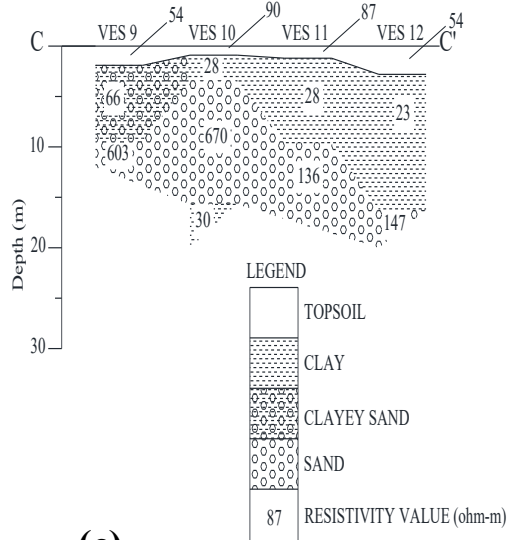
The result from the 2D Wenner array profiles for Alaba indicated that the soil was highly impacted by e-waste. The finding was based on three profiles that were obtained from the dumpsite. Pro-

file 1 (see Fig. 4) was to the north of the dumpsite along Alaba F-Line Locality 1 (see Fig. 1). Two impacted zones of very low resistivity value of  $5 \Omega \cdot m$  were observed. The first zone starts from the ground surface and migrated to about 5 m depth at a lateral distance up to 45 m. The low value of resistivity at the end of the spectrum revealed the real nature of the contaminant plume. The second highly impacted zone spread at a lateral distance of about 83 – 155 m on the topsoil and then increasingly percolates the soil through a narrow gauge between a lateral distance of about 8– 105 m reaching a depth of more than 30 m.

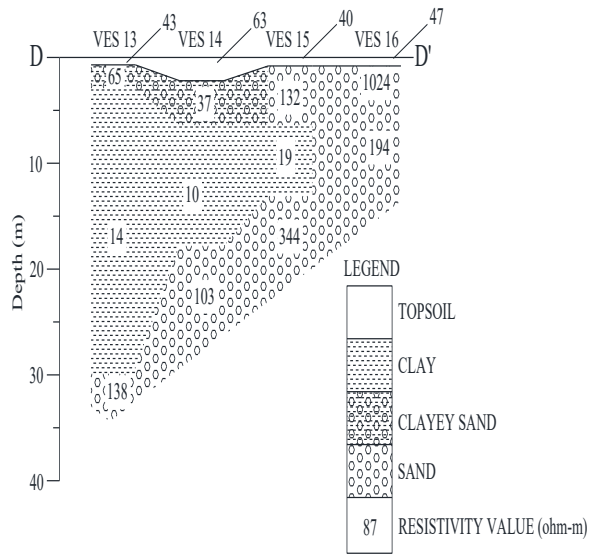


(b)

(a)



(c)



(d)

Figure 3 (a- d): Goelectric Sections of Alaba Dumpsite

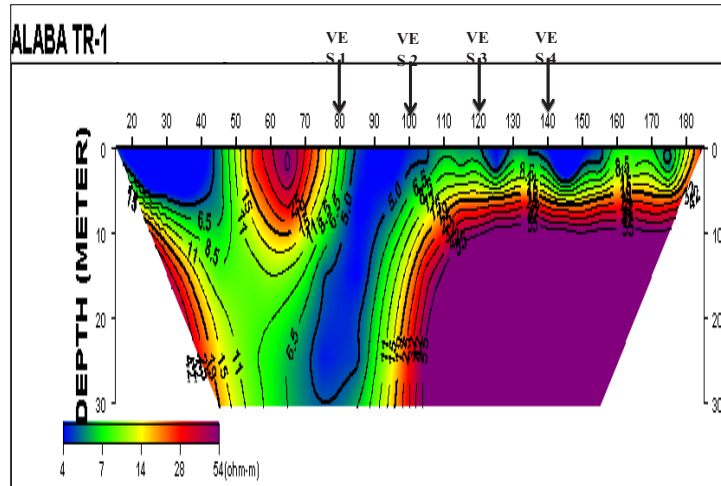


Figure 4: 2D Wenner for Alaba (profile 1)

Profile 2 (see Fig. 5) was to the southern flank of the dumpsite along Alaba F-Line Locality 2 (see Fig. 1) where two impacted zones were also identified. The first, highly impacted zone of low resistivity values of 5.0 - 8.3  $\Omega$ -m lies at a lateral distance of about 10 - 50 m and occupied the sand column of the subsurface as shown by VES 5 and 6 rights in the middle of the dumpsite and on

active locations of e-waste dumping activities. The impacted zone lies at a depth of about 3 m to more than 15 m. Further to the east of the dumpsite at a lateral distance of 73 - 90 m, lies the second slightly impacted zone of 11  $\Omega$ -m resistivity value. The zone lies at a depth range of 6 - 13 m within the sand column subsurface (VES 7).

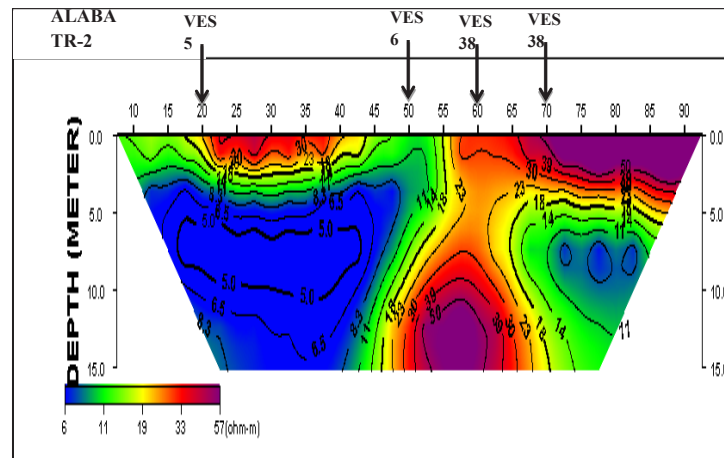


Figure 5: 2D Wenner for Alaba (profile 2)

Profile 3: The profile (see Fig. 6) was further north of the dumpsite along Bishop Mathew Street. The area formed part of the dumpsite before it was built up for residential purpose. The profile indicates two impacted zones. The first zone of low resistivity value between 6.5 and 8.3  $\Omega$ -m was observed at a lateral distance of about 50 - 85 m and progressively increases in depth through the

clayey sand from about 5 - 20 m (VES 14). The second zone of low resistivity value between 5.0 and 8.3  $\Omega$ -m was observed at a lateral distance of about 145 m to more than 180 m. The contaminant progressively increases in depth through the sand column subsurface from about 8 m to more than 30 m (VES 16).



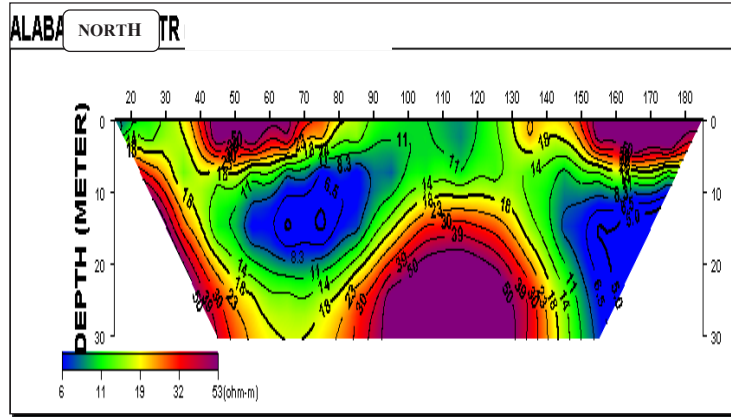
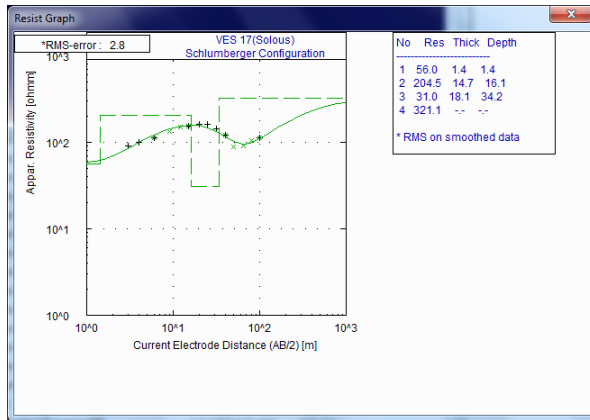


Figure 6: 2D Wenner for Alaba (profile 3)

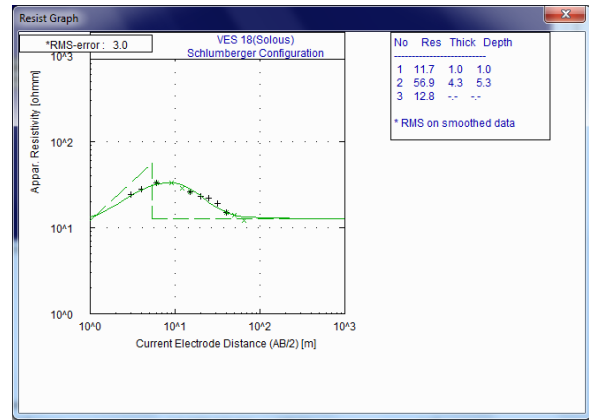
### Goelectric Section (VES) of Soulous Dumpsite Soil

Sounding curve types obtained at Soulous were KH, K, HK, H, AK, and A (see Fig. 7 and Table 3). The iteration of these curve

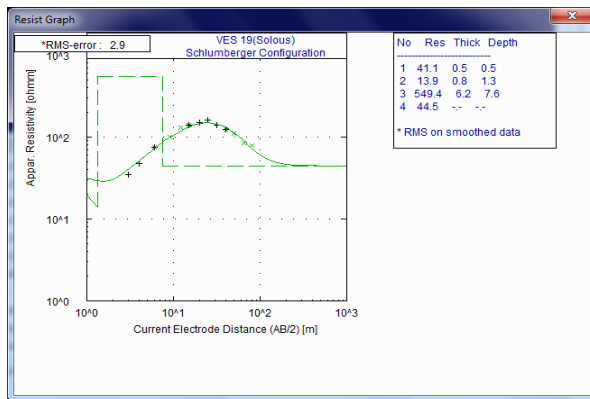
types led to the identification of the geoelectrical section or nature of the dumpsite subsurface soil.



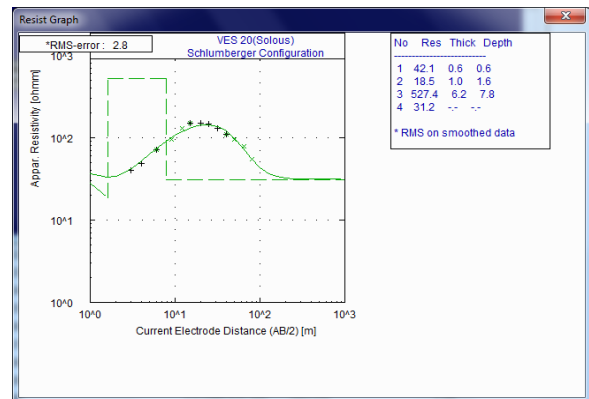
VES 17: KH type:  $\rho_1 > \rho_2 > \rho_3 < \rho_4$  curve



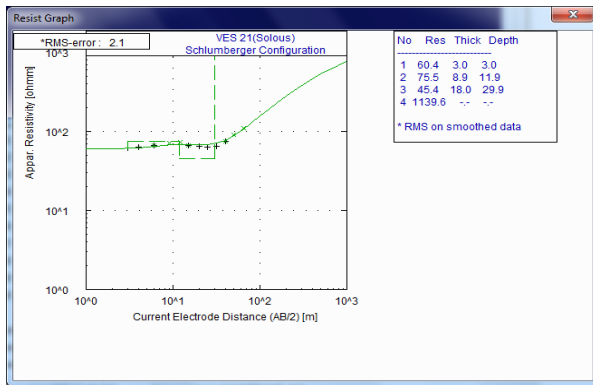
VES 18: K type:  $\rho_1 < \rho_2 > \rho_3$  curve



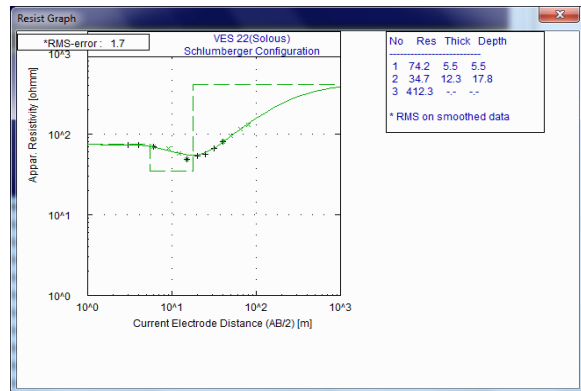
VES 19: HK type:  $\rho_1 > \rho_2 < \rho_3 > \rho_4$  curve



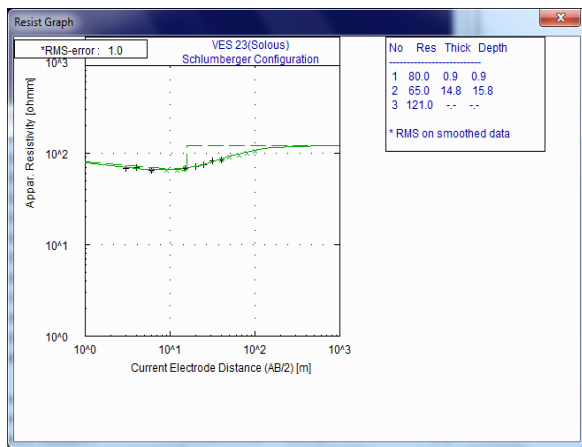
VES 20: HK type:  $\rho_1 > \rho_2 < \rho_3 > \rho_4$  curve



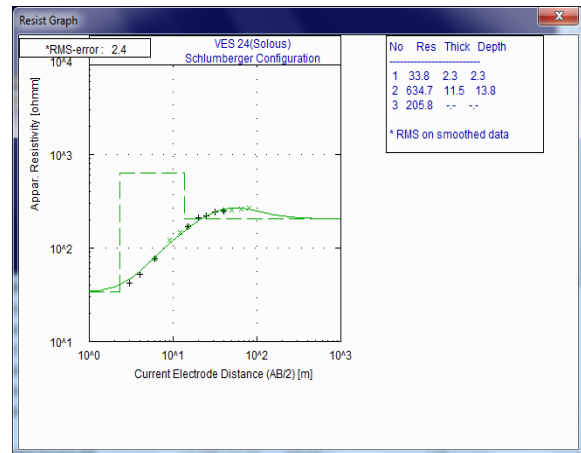
VES 21: KH type:  $\rho_1 > \rho_2 > \rho_3 < \rho_4$  curve



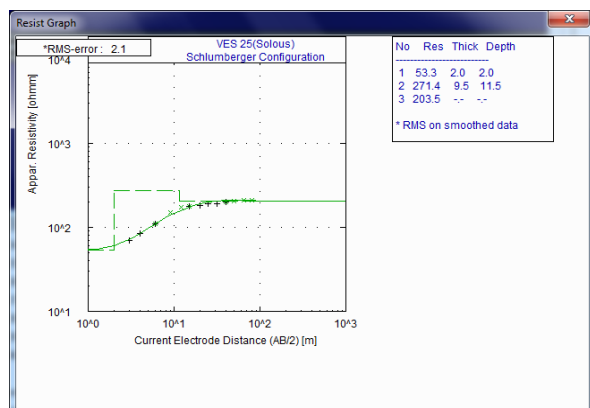
VES 22: H type:  $\rho_1 > \rho_2 < \rho_3$  curve



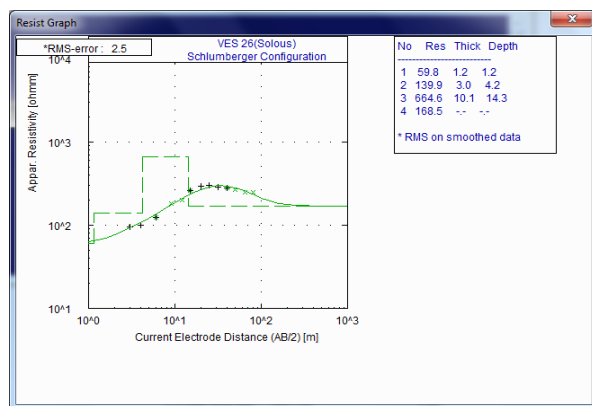
VES 23: H type:  $\rho_1 > \rho_2 < \rho_3$  curve



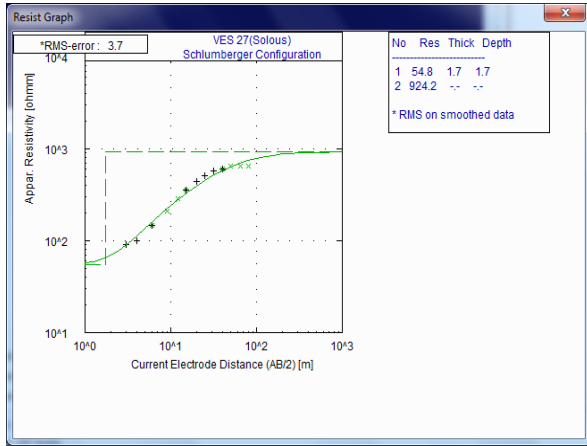
VES 24: K type:  $\rho_1 < \rho_2 > \rho_3$  curve



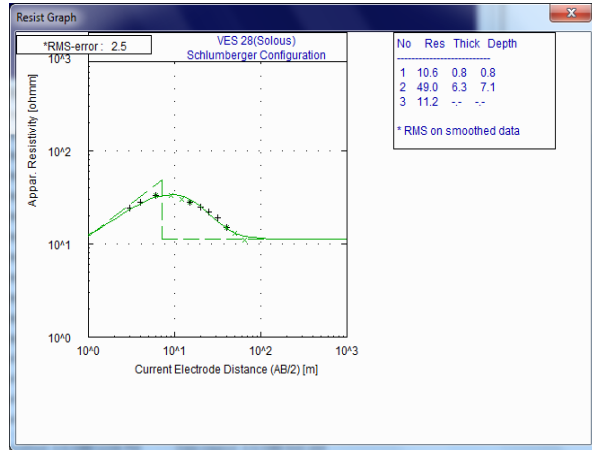
VES 25: A type:  $\rho_1 < \rho_2 < \rho_3$  curve



VES 26: K type:  $\rho_1 < \rho_2 > \rho_3$  curve



A type:  $\rho_1 < \rho_2 < \rho_3$  curve

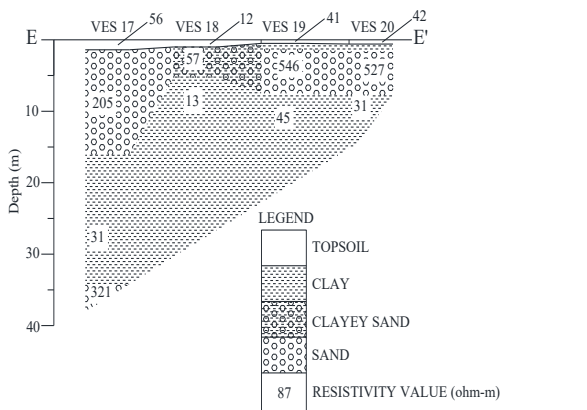


K type:  $\rho_1 < \rho_2 > \rho_3$  curve

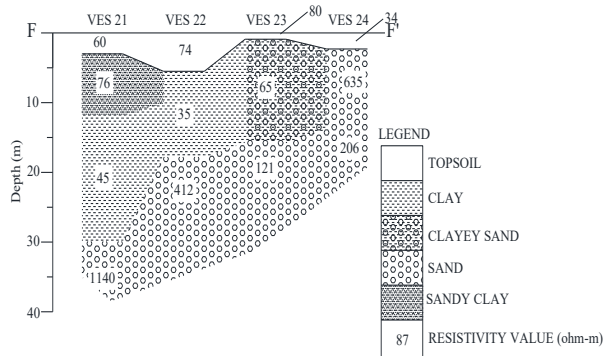
**Figure 7: Solous dumpsite VES curves (VES 17 – VES 28)**

The iteration of the curve types (see Figure. 8 a, b & c) revealed that the geoelectric section of Solous dumpsite consisted mostly four subsurface layers composed of clay column and clay

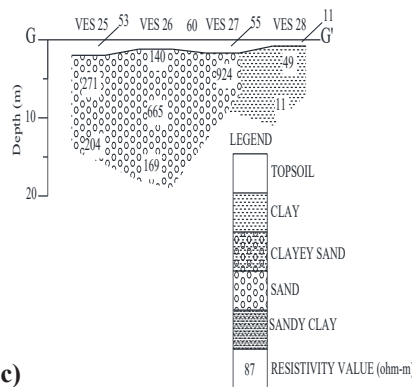
sand in some locations which allowed a low level of impact of the dumpsite soil. The summary of the curve types (VES 17 – VES 28) and site lithology is shown in Table 3.



(a)



(b)



(c)

**Figure 8 (a, b & c): Geoelectrical Sections of Solous Dumpsite**

**Table 3: Vertical Electrical Sounding Summary of Soulous Dumpsite**

VES NO	RESISTIVITY (ohm-m)	THICKNESS (m)	DEPTH (m)	LITHOLOGY	CURVE TYPE
VES 17	56	1.4	1.4	Topsoil	KH
	205	14.7	16.1	Sand	
	31	18.1	34.2	Clay	
	321	-----	-----	Sand	
VES 18	12	1.0	1.0	Topsoil	K
	57	4.3	5.3	Clay	
	13	-----	-----	Clay	
VES 19	41	0.5	0.5	Topsoil	
	14	0.8	1.3	Clay	
	549	6.2	7.6	Sand	
	45	-----	-----	Clay	
VES 20	42	0.6	0.6	Topsoil	HK
	19	1.0	1.6	Clay	
	527	6.2	7.8	Sand	
	31	-----	-----	Clay	
VES 21	60	3.0	3.0	Topsoil	KH
	76	8.9	11.9	Sandy clay	
	45	18.0	29.9	Clay	
	1140	-----	-----	Sand	
VES 22	74	5.5	5.5	Topsoil	H
	35	12.3	17.8	Clay	
	412	-----	-----	Sand	
VES 23	80	0.9	0.9	Topsoil	H
	65	14.8	15.8	Clayey sand	
	121	-----	-----	Sand	
	34	2.3	2.3	Clay	
VES 24	635	11.5	13.8	Sand	K
	206	-----	-----	Sand	
VES 25	53	2.0	2.0	Topsoil	K
	271	9.5	11.5	Sand	
	204	-----	-----	Sand	
VES 26	60	1.2	1.2	Topsoil	A
	140	3.0	4.2	Sand	
	665	10.1	14.3	Sand	
	169	-----	-----	Sand	
VES 27	55	1.7	1.7	Topsoil	A
	924	-----	-----	Sand	
VES 28	11	0.8	0.8	Topsoil	K
	49	6.3	7.1	Clay	
	11	-----	-----		
VES 29	56				HK

## Depths and Spread of Pollutants in Soulous Dumpsite Soil (2D Wenner Array)

The type of subsurface soil determines the rate of percolation as well as the depth and spread of the pollutants in the soil. Thus, the result from the the 2D Wenner array profiles for Soulous indicated that the level of soil impact was low. The finding was based on three profiles that were obtained from the dumpsite as follows:

**Profile 1:** The profile (see Fig. 9) was to the western edge of the dumpsite. An impacted zone of very low resistivity value which ranged from 6  $\Omega\cdot m$  to 11  $\Omega\cdot m$  was observed. The zone started from the ground surface to about 2 m depth, at a lateral distance of 65 – 84 m. The low value of resistivity at the end of the spectrum revealed the real nature of the contaminant plume. Also observed was a no impact zone of 70  $\Omega\cdot m$  resistivity value. The zone dominated a lateral distance from about 30 – 85 m at about 5 m to more than 15 m depth. The relatively high resistivity value spectrum corresponded to the clay column identified in the geoelectric section of VES 18, 19 and 20.

**Profile 2:** The profile (see Fig. 10) was to the east side of the dumpsite. The profile indicated two impacted zones of moderately low resistivity values from 20 - 26  $\Omega\cdot m$ . The first one emanated at a lateral distance of about 60 m and progressively increased in depth from the surface to about 2 m within the next 5 m (i.e at 65 m). The zone could be attributed to the migrating plume from Traverse 1 in Profile 1 (see Fig. 9), suggesting the west – east flow of the plume. The second impacted zone was very pronounced and it occurred at a lateral distance of about 90 – 120 m; at a depth range from 15 m to more than 30 m. Also identified was a zone of no impact with values of resistivity between 141 and 180  $\Omega\cdot m$ . It originated from the ground surface into a depth of more than 30 m. Presumably, the value could be a true representation of the clay subsurface, overlying from Traverse 1 in Profile 1 and in agreement with the geoelectric section of VES 21 and 22.

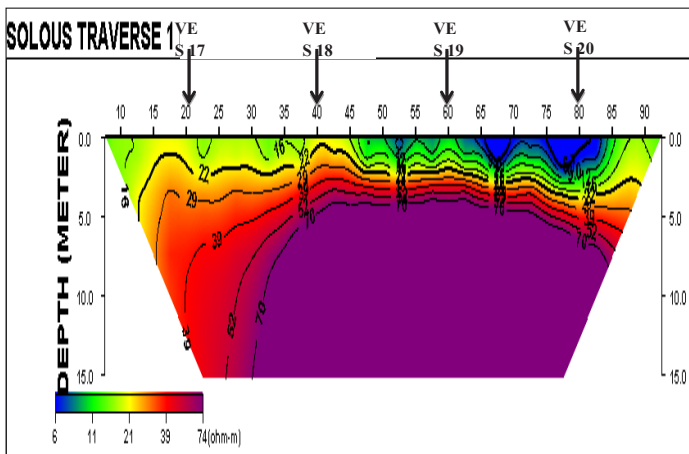


Figure 9: 2D Wenner for Soulous (Profile 1)

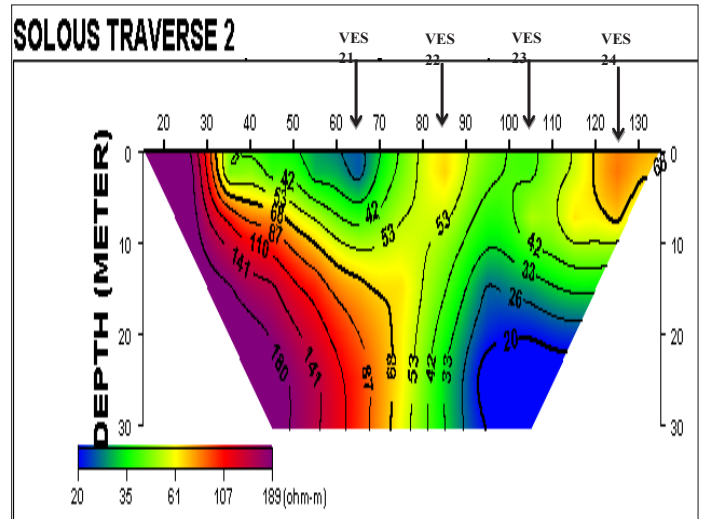


Figure 10: 2D Wenner for Soulous (profile 2)

**Profile 3:** The profile (see Fig. 11) was to the south of the dumpsite. The profile indicated two impacted zones with values of resistivity varying from 40 - 52  $\Omega\cdot m$ . The first one emanated at a lateral distance of about 10 – 30 m and progressively increased in depth from the surface but narrowing in width as it percolated through the sandy subsurface indicated by VES 25 and 26 to a depth of about 7 m. The zone could be linked to the migrating plume from the end of Traverse 2 in Profile 2 (see Fig. 10) and it affirmed the west – east flow of the plume.

Two zones of high resistivity values between 370 and 400  $\Omega\cdot m$  were also observed. The zones were regarded as no impact zones. The first zone lied at a lateral distance between 22 and 45 m while the second zone lied between 68 m and 85 m. The two zones emanated at a depth from about 5 m to more than 15 m in agreement with the true resistivity of the clay subsurface (VES 27 and 28).

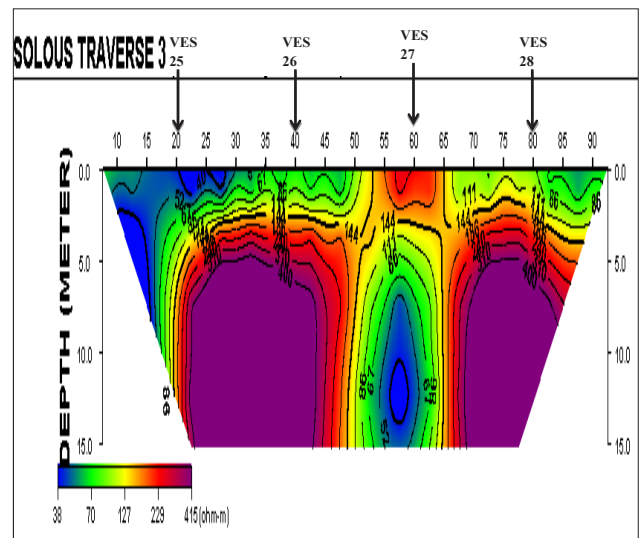


Figure 11: 2D Wenner for Soulous (Profile 3)



---

## Conclusion

The results of the geophysical investigation conducted at Alaba International Market and Soulous-Igando showed that Alaba subsurface soil has been highly impacted as a result of e-waste dumpsite located in the area and more importantly due to the permeable geoelectric characteristics of the lithologic units beneath the dumpsite. The geoelectric sequence is in agreement with the findings of Bello et al., that the sequence consists of sediment of clay, unconsolidated sands and mud with a varying proportion of vegetable matter along the coastal areas while the alluvial deposit consisted of coarse claying unsorted sand with clay lenses and occasional pebble beds [16]. The lithology enables the pollutants to spread laterally and progressively increase in depth through the sand column subsurface to more than 30 m.

Generally, the geophysical study of Soulous dumpsite recorded relatively high resistivity values which correspond to the clay column identified in the geoelectric sections of the site (Fig. 8), thus the level of soil impact was, therefore, low (Fig. 9, 10 & 11). According to Oladapo et al., the clay/laterite column of the subsurface of Igando (Soulous) landfill provides a means of preventing leachate movement down to the aquifer [17].

However, the study found that there was a column of sandy subsoil as shown by VES 22, 23 and 24 (Fig. 8b) through which the west – east flow of the migrating plume had percolated at a depth that ranged from 15 m to more than 30 m on the eastern flank of the dumpsite (Fig 10). In the future, therefore, boreholes/wells dug on this side of the dumpsite might not be totally protected from pollutants.

In conclusion, the study revealed a progressive increase in depth and spread of contaminants into subsurface soil of Alaba. Its three subsurface layers which composed of clay column, clayey sand and sand allows a high level of impact of the dumpsite soil but Soulous-Igando was less impacted because of the nature of the subsurface soil which consists mainly of clay intercalated with lateritic clay

This study provides information on e-wastes as a major environmental problem in Lagos, Nigeria due to the large influx of e-wastes into open dumpsites in the city. The sites are highly populated with wells and boreholes as the main sources of water for the community and so might need to be recovered in the future for a better developmental project. Knowing the difference in the levels of impact of one site compared to the other will allow appropriate decisions on how to detoxify the sites. In addition, the results from this study could facilitate Lagos State Government decisions on the appropriate protection method for groundwater resources around the study areas.

## Declarations

### Availability of Data and Materials

All data generated or analyzed during this study are included in this published article.

## Competing interests

The authors declare that they have no competing interests.

## Funding

Not applicable.

## Authors' contribution

SE reviewed the data analysis. OL reviewed the survey questionnaire and manuscript. All authors read and approved the final manuscript.

## Acknowledgements

The authors wish to thank all Field Assistants and others who participated in the study.

## Authors' information

Not applicable

## References

1. Li, X., Liu, L., Wang, Y., Luo, G., Chen, X., Yang, X., ... & He, X. (2013). Heavy metal contamination of urban soil in an old industrial city (Shenyang) in Northeast China. *Geoderma*, 192, 50-58.
2. Ranieri, E., Fratino, U., Petruzzelli, D., & Borges, A. C. (2013). A comparison between *Phragmites australis* and *Helianthus annuus* in chromium phytoextraction. *Water, Air, & Soil Pollution*, 224(3), 1-9.
3. Balseiro-Romero, M., & Baveye, P. C. (2018). Book Review: *Soil Pollution: A Hidden Danger Beneath our Feet*. *Frontiers in Environmental Science*, 6, 130.
4. Wiczorek, J., Baran, A., Urbański, K., Mazurek, R., & Klimowicz-Pawlas, A. (2018). Assessment of the pollution and ecological risk of lead and cadmium in soils. *Environmental geochemistry and health*, 40(6), 2325-2342.
5. Jiao, X., Teng, Y., Zhan, Y., Wu, J., & Lin, X. (2015). Soil heavy metal pollution and risk assessment in Shenyang industrial district, Northeast China. *PloS one*, 10(5), e0127736.
6. Ofudje, E. A., Akiode, O. K., Oladipo, G. O., Adedapo, E. A., & Adebayo, L. O. (2015). Discharge of Cr, Mn, Ni, Cu and Zn from E-waste Components into Dumpsites Soil at Westminster Market, Lagos Nigeria. *American Chemical Science Journal*, 7(2), 129-138.
7. Adeyi, A. A., & Oyeleke, P. (2017). Heavy metals and polycyclic aromatic hydrocarbons in soil from e-waste dumpsites in Lagos and Ibadan, Nigeria. *Journal of Health and Pollution*, 7(15), 71-84.
8. Akiyode, O. O., & Sojinu, O. S. (2006, March). Assessment of private sector participation (PSP) in solid waste management practices in Nigeria (case study of Lagos State, Nigeria). In *Proceedings of the Twenty first International Conference on Solid Waste Technology and Management*, *Journal of Solid Waste Technology and Management*, Philadelphia, PA USA March (pp. 26-29).
9. Adewumi, B., Akingunsola, E., Femi-Oloye, O. P., & Oloye, F. F. (2017). Evaluation of the Heavy Metals Composition of Soil at E-waste Dumping Sites. *Asian Journal of Environment & Ecology*, 5(4), 1-8.
10. AJAKAYE, P. A., Somoye, E., & Owolabi, L. (2021). Geo-

- 
- physical Assessment of Impact of E-Waste Pollutants on the Subsurface Soil of Alaba International Market Dumpsite in Lagos, Nigeria.
11. Akinlalu, A. A., & Afolabi, D. O. (2018). Borehole depth determination to freshwater and well design using geophysical logs in coastal regions of Lagos, southwestern Nigeria. *Applied Water Science*, 8(6), 1-17.
  12. Odukoya, A. M. (2015). Geochemical and quality assessment of groundwater in some Nigerian basement complex. *International journal of environmental science and technology*, 12(11), 3643-3656.
  13. Coker, J. O. (2012). Vertical electrical sounding (VES) methods to delineate potential groundwater aquifers in Akobo area, Ibadan, South-western, Nigeria. *Journal of Geology and Mining Research*, 4(2), 35-42.
  14. Anudu, G. K., Essien, B. I., & Obrike, S. E. (2014). Hydrogeophysical investigation and estimation of groundwater potentials of the Lower Palaeozoic to Precambrian crystalline basement rocks in Keffi area, north-central Nigeria, using resistivity methods. *Arabian Journal of Geosciences*, 7(1), 311-322.
  15. Vasantrao, B. M., Bhaskarrao, P. J., Mukund, B. A., Baburao, G. R., & Narayan, P. S. (2017). Comparative study of Wenner and Schlumberger electrical resistivity method for groundwater investigation: a case study from Dhule district (MS), India. *Applied Water Science*, 7(8), 4321-4340.
  16. Bello, I. A., Najib, M. U., Umar, S. A., & Ibrahim, G. G. (2015). Measurement of natural radioactivity concentration at E-waste dumpsite around Alaba international market Lagos, Nigeria. *Adv. Appl. Sci. Res*, 6(6), 55-64.
  17. Oladapo, M. I., Adeoye-Oladapo, O. O., & Adebobuyi, F. S. (2013). Geoelectric study of major landfills in the Lagos Metropolitan Area, Southwestern Nigeria. *International journal of water resources and environmental engineering*, 5(7), 387-398.

*Copyright: ©2022 Paul Adeniran Ajakaye. This is an open-access article distributed under the terms of the Creative Commons Attribution License, which permits unrestricted use, distribution, and reproduction in any medium, provided the original author and source are credited.*